Biogeochemistry (2012) 107:227–239
DOI 10.1007/s10533-010-9547-x

Spatial heterogeneity of understory vegetation and soil in an Alaskan upland boreal forest fire chronosequence

M. Lavoie · M. C. Mack

Received: 16 February 2010 / Accepted: 31 October 2010 / Published online: 20 November 2010

Abstract In this study we characterized spatial heterogeneity of soil carbon and nitrogen pools, soil moisture, and soil pH of the first 15 cm of the soil profile; depth of the organic horizon; forest floor covers; and understory vegetation abundances in three sites (1999, 1987 and 1920 wildfires) of a boreal forest chronosequence of interior Alaska. We also investigated the cross-dependence between understory vegetation distribution and soil characteristics. Our results showed higher microbial respiration rates and microbial biomass in the oldest site and greater net N mineralization rates in the mid-successional site. Although spatial heterogeneity was absent at the scale studied for the majority of soil variables (60%), understory vegetation abundances and forest floor cover, spatial heterogeneity decreased with time after fire for the depth of organic horizon, soil microbial biomass, N mineralization rates and feathermoss cover. Our results also showed that increasing time after fire decreased the number of correlations between understory vegetation and soil characteristics while it increased between forest floor covers and soil characteristics. Overall, our study suggest that fire initially creates a patchy mosaic of forest floor cover, from fire hot spots, where high intensity burning exposes mineral soil, to practically unburned areas with intact mosses and lichens. As time since fire passes, forest floor cover and soil characteristics tend to become more uniform as understory species fill in severely burned areas.

Keywords Alaska · Boreal forest · Carbon · Nitrogen · Spatial analysis · Wildfire

M. Lavoie (✉) · M. C. Mack
Department of Biology, University of Florida,
220 Bartram Hall, Gainesville, FL 32611, USA
e-mail: martin21skifond@gmail.com

Introduction

The heterogeneity of soil nutrient availability is often associated with variation in plant distribution (Vinton and Burke 1995; Schlesinger et al. 1996; Stoyan et al. 2000; Hirobe et al. 2001). In communities undergoing secondary succession, the spatial heterogeneity of soil processes and vegetation may change over time (Ryel et al. 1996; Ehrenfeld et al. 1997; Cain et al. 1999) due to the direct effects of the disturbance on soil properties (Robertson et al. 1993; Hirobe et al. 2003; Blair 2005; Gundale et al. 2006), the indirect effects of the disturbance on plant composition and distribution (Gross et al. 1995), and interactions between plants and soils (Hirobe et al. 2003; Gallardo et al. 2005).

In boreal forests, wildfire is an important driver of vegetation succession (Degrandpre et al. 1993; Viereck et al. 1983; Mack et al. 2008) and soil nutrient cycling (Smith 1970; Dyrness et al. 1989).

Fire may partially or completely consume organic soil layers (Boby et al. 2010), creating heterogeneity in residual soil characteristics that control nutrient cycling. Fires in many parts of the boreal forest tend to be stand replacing (Kasischke 2000), although understory species of vascular plants may re-sprout after fire depending on the depth of burning (Chapin et al. 2006). Although fire has clear effects on both soil properties and plant distributions, we know little about the effects of fire on the spatial heterogeneity of those two components and how they may interact over post-fire succession (see Fortin et al. 1999; Bond-Lamberty et al. 2006). In this study we characterized spatial heterogeneity of soil processes, plant composition and their interactions along an Alaskan fire chronosequence. We assessed soil carbon (C) and nitrogen (N) pools, gravimetric soil moisture, and pH, forest floor cover and depth of the organic horizon, and the abundance of understory vegetation. We established whether the spatial heterogeneity of each variable changed with time since fire. Lastly, we determined if there was a cross-dependence within, among and between all variables. Since we were particularly interested in the interactions between soil and plants, we concentrated our soil analysis on the first 15 cm of the soil profile, the area with the highest density of fine roots.

While there are numerous metrics used to quantify spatial heterogeneity, we used the semivariogram because of its ease of interpretation and its wide use in the literature (Rossi et al. 1992; Dormann et al. 2007). In this study, we defined spatial heterogeneity as the integration of two elements: global variability and patchiness. For example, a soil property from a study site will be considered more heterogeneous if it has higher global variation (higher coefficient of variation) and finer patch size (smaller semivariogram ranges) than the other study sites. As a result, we hypothesized that the spatial heterogeneity of soil C and N pools and depth of the organic horizon would decrease with time since fire. We also hypothesized that fire would affect spatial heterogeneity of the understory vegetation cover as composition changed over time after fire, from smaller patches of forbs and grasses to larger patches of ericaceous shrubs and mosses. We also expected a low degree of correlation between soil nutrient pools and vegetation abundance due to a relatively low understory cover and low vegetation patchiness.

Materials and methods

Study sites

We carried out our study on three established sites on a fire chronosequence in upland boreal forests of the Donnelly Flat areas, located approximately 140 km southeast of Fairbanks near Delta Junction (63°55′N; 145°44′W) in interior Alaska. Sites had been burned in severe fires during the summer of 1999 (F99), 1987 (F87) and 1920 (F20) (Treseder et al. 2004, 2007; Liu et al. 2005; Mack et al. 2008). The oldest site (1920 fire, hereafter F20), is dominated by black spruce (*Picea mariana*). The intermediate-aged site (1987 fire, hereafter F87), is dominated by trembling aspen (*Populus tremuloides*) and black spruce. The youngest site (1999 fire, hereafter F99) was dominated, prior to fire, by black spruce but is now populated by graminoids and trembling aspen (Table 1). Litter, lichens and mosses (*Pleurozium schreberi* and *Hylocomium splendens*) cover the forest floor of the F20 site (Table 2). The forest floor in the F87 site was covered with litter and *Ceratodon purpureus* while the recent fire (F99) was mainly covered with *C. purpureus*, bare mineral soil and litter. Understory cover in the the F99 and F87 sites was very scarce while the F20 site was composed of black spruce and ericaceous shrubs (Table 2).

All sites are located within a 100 km^2 landscape on gently sloped alluvial soils that range from moderately well-drained soils to well-drained soils with elevations of approximately 500 m above sea level (Treseder et al. 2004; Liu et al. 2005). Sites from this study were all located on well-drained soils where permafrost was not present (Mack et al. 2008). Soils in all sites are gelisols formed from loessal inputs carried by sediments of the Tanana River (Richter et al. 2000). Silt loams predominate, underlain by deposits of sand and gravel. The regional climate is cold and dry, with a mean annual temperature of −2°C and a precipitation rate of 303 mm $year^{-1}$ (http://weather.noaa.gov/). The growing season typically lasts from budbreak in May to leaf senescence in September.

Sampling design

In June 2007, we randomly located a 400 m^2 plot (20 m × 20 m) in each site. In each plot, we established a systematic grid for soil sampling and

Table 1 Site characteristics for a boreal forest chronosequence in interior Alaska

	1999 Wildfire	1987 Wildfire	1920 Wildfire
Stem density (stem ha^{-1})			
Picea mariana	2600[a]	5950	4675
Populus tremuloides	200	6225	–
Regeneration density (stem ha^{-1})			
Picea mariana	600	3159	1500
Populus tremuloides	200	2500	–
Tree basal area (m^2 ha^{-1})			
Picea mariana	5.1[a]	0.12	11.0
Populus tremuloides	–	6.2	–
Mean tree DBH (cm)			
Picea mariana	4.1	1.3	4.5
Populus tremuloides	–	4.8	–

[a] Dead trees (snags)

Table 2 Forest floor cover characteristics and understory vegetation abundance for a boreal forest chronosequence of interior Alaska ($n = 81$ samples per site)

	1999 Wildfire		1987 Wildfire		1920 Wildfire	
	Mean (%)	CV (%)	Mean (%)	CV (%)	Mean (%)	CV (%)
Forest floor cover (%)						
Lichen cover	0.0b	–	3.7b	160.6	35.8a	79.8
Moss cover						
Polytrichum spp.	2.2a	456.0	2.3a	247.0	0.1a	900.0
Pleurozium schreberi	0.0b	–	0.0b	–	6.7a	266.0
Hylocomium splendens	0.0b	–	0.0b	–	30.0a	107.0
Dicranum spp.	0.0b	–	0.0b	–	1.2a	268.0
Ceratodon purpureus	73.0a	34.0	28.0b	86.0	0.0c	–
Litter cover	8.6c	210.0	66.1a	38.5	16.1b	126.0
Mineral soil cover	16.1a	121.1	0.3b	900.0	0.0b	–
Understory vegetation (%)						
Picea mariana	0.0b	632	3.3b	322.6	15.2a	113.5
Populus tremuloides	0.1b	900	2.1a	218.0	0.0b	0.0
Salix spp.	3.7a	320.7	0.9b	468.5	0.0b	0.0
Vaccinium vitis-idaea	3.5b	149.7	2.3b	265.7	24.7a	63.5
Vaccinium uliginosum	1.7a	387.7	1.8a	354.1	1.0a	325.9
Ledum groenlandicum	0.9a	679.6	2.2a	362.4	4.8a	200.7
Ledum palustre	1.1a	357.3	0.0b	0.0	0.0b	0.0
Festuca altaica	17.2a	111.9	0.2b	667.5	2.3b	296.0

Different letters denote significant differences between sites ($p < 0.05$)

vegetation assessment. Each grid was divided into hundred 2.0 m × 2.0 m grid cells (Fig. 1). Sampling points were located systematically at 41 of the grid intersections following Havorton et al. (1995) and Guo et al. (2004). Within each large plot, two 2.0 m × 2.0 m grid cells were randomly chosen to contain an additional 20 sampling point each (i.e., total of 81 sampling points for each plot). The point layout in these smaller plots was similar to that of the larger scale plots, except the minimum distance between points was 0.5 m rather than 2.0 m.

At each sampling location, from the surface a 0–15 cm depth volumetric soil sample was taken with a 4.5 cm diameter soil core. For this study we concentrated on the 0–15 cm depth because it is the area with the highest density of fine roots

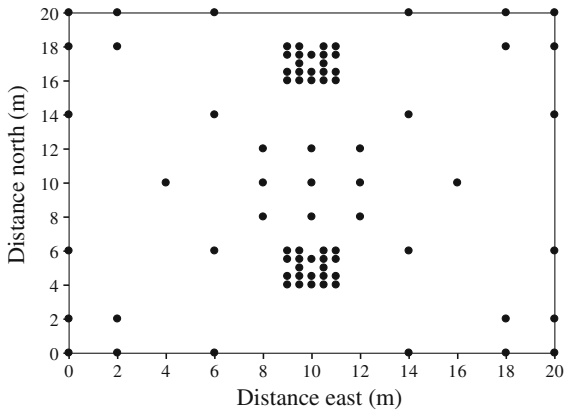

Fig. 1 Schematic layout of survey plots used to measure spatial structure of understory vegetation and soil characteristics on a boreal fire chronosequence

(Van Cleve et al. 1983). Soil samples were kept on ice for transport back to University of Alaska in Fairbanks and kept at 4°C until processing. Soil processing occurred within 2 weeks at the University of Florida in Gainesville, Florida.

At each sampling point, we also measured the depth of the organic layer and buried a mixed-bed resin bag at ca. 5 cm deep to assess resin-available fluxes of inorganic N. All resin bags were retrieved 15 August 2007. In a 0.25 m^2 (50 cm × 50 cm) quadrat centered on each soil sampling point, we assessed percent cover of vegetation and forest floor by species or substrate.

Soil analysis

Soils were homogenized and roots, twigs, and green vegetation were removed by hand. From each soil sample ($n = 81$ per plot), a sub-sample was used to determine gravimetric moisture content, total C and N, initial inorganic nitrogen (NO_3^-–N and NH_4^+–N), initial basal respiration, initial soil microbial biomass and pH. Inorganic nitrogen, soil basal respiration and soil microbial biomass were also measured after a 3-month aerobic laboratory incubation at field moisture and 15°C.

Soil respiration and soil microbial biomass

To determine basal respiration at each sample point, we placed one specimen cup filled with approx. 40–50 g fresh weight soil into one 1 l Mason jar. We measured CO_2 production from the samples by sealing the Mason jars and measuring CO_2 accumulation in the headspace over a 48 h period. Air spaces (10 ml) were taken at time 0 and at 48 h by syringe through a septum in the Mason jar lid, and injected into a Li-Cor (Li-Cor, Ne, USA). Carbon dioxide production was expressed as μg C gdw^{-1} h^{-1}.

Soil microbial biomass was determined with the substrate-induced-respiration (SIR), which consists of measuring the rate of initial maximal respiration of microorganisms after amendment of soil subsamples with glucose (Anderson and Domsch 1978). Soil samples (approx. 1 g fresh weight) were placed in a vial (25 ml) and a glucose solution was added dropwise (10 mg glucose g^{-1} soil, volume was 0.1 ml). Soil samples were incubated for 2 h at 22°C. Head space gas samples were collected and CO_2 production was determined using a Li-Cor. Soil microbial biomass (C_{mic}) was derived by the SIR measurement according to the equation: C_{mic} (μg C g^{-1} soil) = (μl CO_2 soil h^{-1}) × 40.04 + 0.37 (Anderson and Domsch 1978).

Inorganic nitrogen and nitrogen mineralization

To determine N mineralization potential, soil samples were analyzed for initial and final pools after 3 months lab incubation of inorganic N (NH_4^+–N and NO_3^-–N) by extracting approximately 20 g of field moist soil with 90 ml of 0.5 M K_2SO_4 (Robertson et al. 1999). The solutions were shaken for 1 h and left to sit in an air-conditioned room (approx. 23°C) for 18–24 h and then filtered using a Whatman (GF/A) filter under vacuum. Ammonium and NO_3^- concentrations in extracts were determined colorimetrically using an Astoria-Pacific colorimetric autoanalyzer (Astoria, OR, USA). Net rates of nitrification and N mineralization for the incubation period were calculated from the differences in initial and final inorganic N pools divided by the incubation time. All initial N pools and N turnover rates were calculated on a dry soil mass basis (e.g., μg N gdw^{-1}).

In addition to determination of N mineralization in the laboratory, we also measured N mineralization in the field using mixed bed resins bags. Field measurements allowed us to quantify the excess of inorganic N available after assimilation by microorganisms and plants. After being retrieved from the field, the mixed bed resin bags were extracted with

2 M KCL. The solutions were shaken for 1 h and left then filtered using a Whatman (GF/A) filter under vacuum. Ammonium and NO_3^- concentrations in extracts were determined colorimetrically using an Astoria-Pacific colorimetric autoanalyzer.

Elemental analysis

Total soil C and N were measured on subsamples of initial soil cores using a Costech ECS 4010 Elemental Analyzer (Valencia, CA). The pH measurements were made in aqueous suspensions (approx. soil:water ratio = 1:5). Total (C and N) were calculated on a dry soil mass basis.

Statistical analysis

Mean, standard error and coefficient of variation were calculated for soil variables, vegetation abundances and forest floor covers. We also examined correlation between and among soil, vegetation and forest floor variables. To include the effects of spatial autocorrelation of data, the differences between sites were tested using a spatially adjusted one-way ANOVA (Proc Mixed with a spatial covariance structure). We also used generalized least squares regressions (GLS; Ives and Zhu 2006; Bugueria and Pueyo 2009; Beale et al. 2010) to evaluate the variation in extractable inorganic nitrogen, laboratory and field N mineralization rates, microbial respiration, and microbial biomass as a function of gravimetric soil moisture, depth of the organic horizon, total N, and total C. All statistical analyses were computed using SAS 9.1 (SAS Institute Inc. 2003) except for GLS regressions, which were performed with R 2.11.1 statistical software (Ellner 2001; R Development Core Team 2010). Data were checked for normality and equality of variance prior to statistical analyses.

Spatial heterogeneity analysis

Semivariogram analysis was used to examine spatial heterogeneity for soil, vegetation abundance (when possible) and the forest floor covers (when possible) (Legendre and Fortin 1989). Data sets that did not visually approximate a normal distribution were natural log transformed and all variables were checked for the presence of a broad spatial trend prior to analysis. The results of the semivariograms were fitted to one of five models: Nugget, Linear, Gaussian, Spherical and Exponential. These fitted models can be classified as exhibiting one of three types of spatial structure: (1) The Nugget model indicated random spatial structure or lack of spatial dependence at the scale studied, (2) The Linear model, in which the variance increases proportionally with lag distance, indicated that the spatial structure may extend beyond the scale sampled, (3) The remaining models (Gaussian, Spherical, Exponential) exhibited asymptotic spatial structure in which the variance becomes constant after a certain lag distance (Legendre and Fortin 1989).

Where possible, we calculated the range of autocorrelation (i.e., statistical term for heterogeneity) or the distance at which sample values are no longer correlated (i.e., where a plateau is reached), the sill ($C + C_o$) or the error variance where samples are no longer correlated, and the nugget (C_o) which is the variance that is not spatially dependent. To estimate the magnitude of spatial dependence, we calculated structural variance, the proportion of the total model variance [$C/(C + C_o)$], as a measure of spatial dependence, or in other words, the percentage of total variance explained by spatial dependence from the available sampling grid (Rossi et al. 1992; Legendre and Legendre 1998; Ettema and Wardle 2002; Outeiro et al. 2008). Structural variance approaches one in a strongly spatially structured system with no nugget semivariance and approaches zero (a pure nugget model) in a system with little structure in the range of scale measured. Each semivariogram was calculated with a minimum of 30 data pairs per distance and with a maximum of half the total distance measured in any direction over the sampling space (Rossi et al. 1992). Semivariograms were performed using GS+ version 9.0 (Gamma Design Software 2008).

Results

Global variation

The depth of the organic horizon increased from 1.6 to 7.8 cm and pH decreased from 5.81 to 5.16 from the young to the old fire scars (Table 3). In contrast, gravimetric soil moisture was higher (69%) in the mid-succession site than the young (59%) or

Table 3 Mean, coefficient of variation (CV) and spatial statistics for pH, gravimetric soil moisture and depth of the organic horizon in a boreal forest chronosequence of interior Alaska

Soil variable	Mean	CV (%)	Model	R^2	Range (m)	$C/(C+C_0)$
1999 Wildfire						
pH	5.81a	0.2	NUG	0.000	–	0.0
Gravimetric soil moisture	58.7ab	38.5	LIN	0.751	–	0.0
Depth of organic horizon (cm)	1.6c	86.0	SPH	0.396	3.7	0.90
1987 Wildfire						
pH	5.59b	0.4	GAU	0.122	1.2	0.27
Gravimetric soil moisture	69.2a	48.3	SPH	0.540	3.3	0.32
Depth of organic horizon (cm)	5.5b	39.1	SPH	0.304	5.3	0.70
1920 Wildfire						
pH	5.16c	0.6	LIN	0.415	–	0.0
Gravimetric soil moisture	55.9b	54.9	SPH	0.564	22.5	0.50
Depth of organic horizon (cm)	7.8a	57.2	EXP	0.545	6.5	0.79

The best-fit model is presented for each variable (*EXP* exponential, *GAU* Gaussian, *SPH* spherical, *LIN* linear, *NUG* nugget). Proportion is defined as the proportion of total variance accounted for by spatially dependent variance ($C/(C+C_0)$) and is an indicator of the magnitude of spatial dependence of each variable. Different letters denote significant differences between sites ($p < 0.05$)

old (56%) sites. The coefficient of variation was larger for the depth of the organic horizon and gravimetric soil moisture than pH. Net N mineralization (in the laboratory and in situ) and extractable N ($NO_3^- + NH_4^+$) were significantly higher in the mid-succession (i.e., F87) site (Table 4) but on a C and N basis (data not shown), net N mineralization in situ was higher in the younger (i.e., F99) site. In contrast, microbial respiration, microbial biomass and the C:N ratio were higher in the older (i.e., F20) site. The coefficient of variation was larger for N (38–445%) (Table 4) than C pools (4–63%) (Table 5) and there was no consistent effect of fire on the coefficient of variation.

Spatial heterogeneity and structural variance

The soil variables did not exhibit a very strong spatial structure in the three sites, suggesting that time after fire did not generally affect the spatial structure of the C and N pools (Tables 4, 5). Time after fire did have an effect, however, on the spatial structure of the depth of the organic horizon, microbial biomass, and N mineralization rates. The range of autocorrelation increased, respectively, from 3.7 to 6.5 m, from 2.0 to 10.7 m, and from <0.5 to 3.3 m with time since fire (Tables 3, 5; Fig. 2). Furthermore, structural variances for the depth of the organic horizon was, across the chronosequence, consistently higher than 70%, suggesting that much of the total variance was a function of spatial autocorrelation. As for the microbial biomass and N mineralization rates, the percentage of the total variance explained by spatial dependence increased with time after fire. The F99 site had only four variables with spatial structure while the F87 and F20 sites had seven and six respectively (Tables 3, 4, 5); all but one had range of autocorrelation under 7 m. Most variables were described by linear or nugget semivariograms, with varying degrees of scatter.

Regarding understory vegetation and forest floor cover, very few species or cover was present in at least 50% of the sampling points for all three sites. As a result, we were able to calculate semivariograms for very few of them. In the F99 site, *Ceratodon purpureus* exhibited a range of autocorrelation of 6 m, while exposure of bare mineral soil exhibited no spatial structure. In the F87 site, *Ceratodon purpureus* had a range of autocorrelation of 2.2 m, whereas the LFH layers showed a shorter range at 0.5 m. In the oldest stand (F20), *Picea mariana* and *Vaccinium vitis-idaea* expressed a range of 3.2 and 4.1 m respectively. *Hylocomium splendens* and the LFH layer had, respectively, a range of autocorrelation of 8.1 and 0.6 m while lichens expressed no sign of spatial structure at the scale studied. Fire decreased the range of autocorrelation only for feathermosses cover: from 2.8 (F99) to 13 m (F20) (Fig. 2g–i).

Table 4 Mean, coefficient of variation (CV) and spatial statistics for nitrogen pools in a boreal forest chronosequence of interior Alaska

Soil variable	Mean (%)	CV (%)	Model	R^2	Range (m)	C/(C+C$_0$)
1999 Wildfire						
Total N (%)	0.30b	37.8	LIN	0.056	–	0.0
Net N mineralization in situ (mg N gdw^{-1} of resin)[a]	3.90a	88.5	NUG	0.031	–	0.0
Net N nitrification in situ (mg N gdw^{-1} of resin)[a]	0.05b	444.7	NUG	0.006	–	0.0
Laboratory N mineralization (μg N gdw^{-1})[b]	3.69b	183.4	LIN	0.111	–	0.0
Extractable N (NO_3^- + NH_4^+; μg N gdw^{-1})	5.64b	70.3	GAU	0.596	1.9	0.80
1987 Wildfire						
Total N (%)	0.37a	41.5	LIN	0.000	–	0.0
Net N mineralization in situ (mg N gdw^{-1} of resin)[a]	3.75a	59.3	NUG	0.073	–	0.0
Net N nitrification in situ (mg N gdw^{-1} of resin)[a]	0.45a	208.4	EXP	0.018	0.5	0.70
Laboratory N mineralization (μg N gdw^{-1})[b]	47.5a	113.1	SPH	0.337	2.3	0.87
Extractable N (NO_3^- + NH_4^+; μg N gdw^{-1})	9.21a	84.9	SPH	0.125	2.9	0.59
1920 Wildfire						
Total N (%)	0.34ab	58.4	NUG	0.012	–	0.0
Net N mineralization in situ (mg N gdw^{-1} of resin)[a]	3.05b	118.8	SPH	0.177	3.3	0.80
Net N nitrification in situ (mg N gdw^{-1} of resin)[a]	NS	ND	ND	ND	ND	ND
Laboratory N mineralization (μg N gdw^{-1})[b]	6.06b	285.4	NUG	0.010	–	0.0
Extractable N (NO_3^- + NH_4^+; μg N gdw^{-1})	5.34b	129.5	LIN	0.155	–	0.0

[a] Accumulation over a 40-day period; [b] Accumulation over a 3-month period; *NS* non significant; *ND* not determined

The best-fit model is presented for each variable (*EXP* exponential, *GAU* Gaussian, *SPH* spherical, *LIN* linear, *NUG* nugget). Proportion is defined as the proportion of total variance accounted for by spatially dependent variance (C/(C+C$_0$)) and is an indicator of the magnitude of spatial dependence of each variable. Different letters denote significant differences between sites ($p < 0.05$)

Pearson correlations and Generalized Least Squares regressions

Nitrogen and C mineralization were significantly correlated to total C and total N (Table 6). Extractable inorganic N, microbial respiration (except F99) and microbial biomass were all correlated to total C and N for the three sites. In contrast, field N mineralization showed no significant correlations for any of the sites. When spatial autocorrelation was taken into account, our result showed that in the 1920 and 1999 fires, 20–30% of the total variation in extractable inorganic N was explained by total C and N, respectively (Table 7). In addition, for the same wildfires, the microbial biomass (initial) was also positively correlated to total C and N, which explained up to 50% of the total variation (Table 7).

The correlations between the understory vegetation and the soil variables (data not shown) were generally low (i.e., $r < 0.5$). However, our results showed that increasing time after fire reduced the number of significant correlations with 18% (27 out of 150 correlation pairs), 9% (13 out of 150 correlation pairs), and 7% (10 out of 135 correlation pairs) for the F99, F87 and F20 sites respectively. Our results also highlighted that increasing time after fire increased the number of significant negative correlations (from 1 to 7). In addition, only the younger sites (F99 and F87) showed correlations between species abundance and extractable inorganic N or in situ and laboratory N mineralization incubations. Four and five species, respectively for the F99 and F87 sites were correlated to extractable N and N mineralization rates, with all the correlations being higher in the F99 than the F87 site. At last, the number of significant correlations between forest floor covers and soil increased with time since fire; from only 3 in F87 and F99 (litter and *Ceratodon purpureus*) to 17 in the F20 site (lichen and feathermosses).

Table 5 Mean, coefficient of variation (CV) and spatial statistics for carbon pools in a boreal forest chronosequence of interior Alaska

Soil variable	Mean (%)	CV (%)	Model	R^2	Range (m)	$C/(C+C_0)$
1999 Wildfire						
Total C (%)	6.99b	41.8	LIN	0.134	–	0.0
CN ratio	22.82c	7.9	LIN	0.259	–	0.0
Microbial respiration (initial) (μg $g^{-1}C\ h^{-1}$)	15.2c	40.4	SPH	0.113	3.1	0.27
Microbial biomass (initial) (μC mic gdw^{-1})	1188.8b	4.2	SPH	0.101	2.0	0.30
Microbial respiration (3 months) (μg C $gdw^{-1}h^{-1}$)	14.1a	45.8	NUG	0.029	–	0.0
Microbial biomass (3 months) (μC mic gdw^{-1})	667.0b	7.2	LIN	0.815	–	0.0
1987 Wildfire						
Total C (%)	9.32a	42.8	LIN	0.092	–	0.0
CN ratio	25.4b	10.24	LIN	0.130	–	0.0
Microbial respiration (initial) (μg $g^{-1}C\ h^{-1}$)	18.8b	38.4	LIN	0.128	–	0.0
Microbial biomass (initial) (μC mic gdw^{-1})	1826.1a	5.7	SPH	0.125	2.9	0.59
Microbial respiration (3 months) (μg C $gdw^{-1}\ h^{-1}$)	13.1a	52.4	LIN	0.002	–	0.0
Microbial biomass (3 months) (μC mic gdw^{-1})	901.3ab	5.7	LIN	0.101	–	0.0
1920 Wildfire						
Total C (%)	11.3a	63.8	NUG	0.033	–	0.0
CN ratio	33.3a	14.8	EXP	0.257	1.8	0.55
Microbial respiration (initial) (μg $g^{-1}C\ h^{-1}$)	26.3a	61.4	LIN	0.178	–	0.0
Microbial biomass (initial) (μC mic gdw^{-1})	1925.4a	8.3	GAU	0.740	10.7	0.68
Microbial respiration (3 months) (μg C $gdw^{-1}\ h^{-1}$)	15.5a	62.6	SPH	0.056	1.0	0.93
Microbial biomass (3 months) (μC mic gdw^{-1})	1172.3a	9.4	LIN	0.334	–	0.0

The best-fit model is presented for each variable (*EXP* exponential, *GAU* Gaussian, *SPH* spherical, *LIN* linear, *NUG* nugget). Proportion is defined as the proportion of total variance accounted for by spatially dependent variance ($C/(C+C_0)$) and is an indicator of the magnitude of spatial dependence of each variable. Different letters denote significant differences between sites ($p < 0.05$)

Discussion

This study showed higher microbial respiration rates and microbial biomass in the oldest sites, where organic matter content, bulk soil C concentration and soil C:N ratio were highest, and greater net N mineralization rates in the mid-successional site, where soil C:N ratios were substantially lower. Our results showed a decrease in spatial heterogeneity with time after fire for the depth of organic horizon, soil microbial biomass, N mineralization rates and feathermoss cover. This study also showed that the correlations between soil characteristics and understory vegetation and forest floor cover changed as time elapsed after fire.

In this Alaskan upland boreal chronosequence, microbial biomass and microbial respiration rates increased with time since fire. This increase may be due the presence of a deeper organic horizon and a higher total C in the oldest site. In contrast, net N mineralization rates and extractable N were higher in the intermediate-aged site, a result consistent with Treseder et al. (2004) for the same fire. The higher N transformation rates and extractable N in the 1987 wildfire is likely due to the accumulation of leaf litter from trembling aspen (Légaré et al. 2005; Kielland et al. 2006), a easily decomposable species (Flanagan and Van Cleve 1983). In contrast, slowly decomposing black spruce and feathermoss litter may be primary responsible for the reduction in N availability and N transformation rates in the oldest site (Flanagan and Van Cleve 1983).

The three sites we selected had the typical structure of an Alaskan dry boreal forest chronosequence, including a strong hardwood component at the mid-successional stage and increasing organic horizon depth and abundance of feathermosses and ericaceous shrubs as time progressed after fire. These

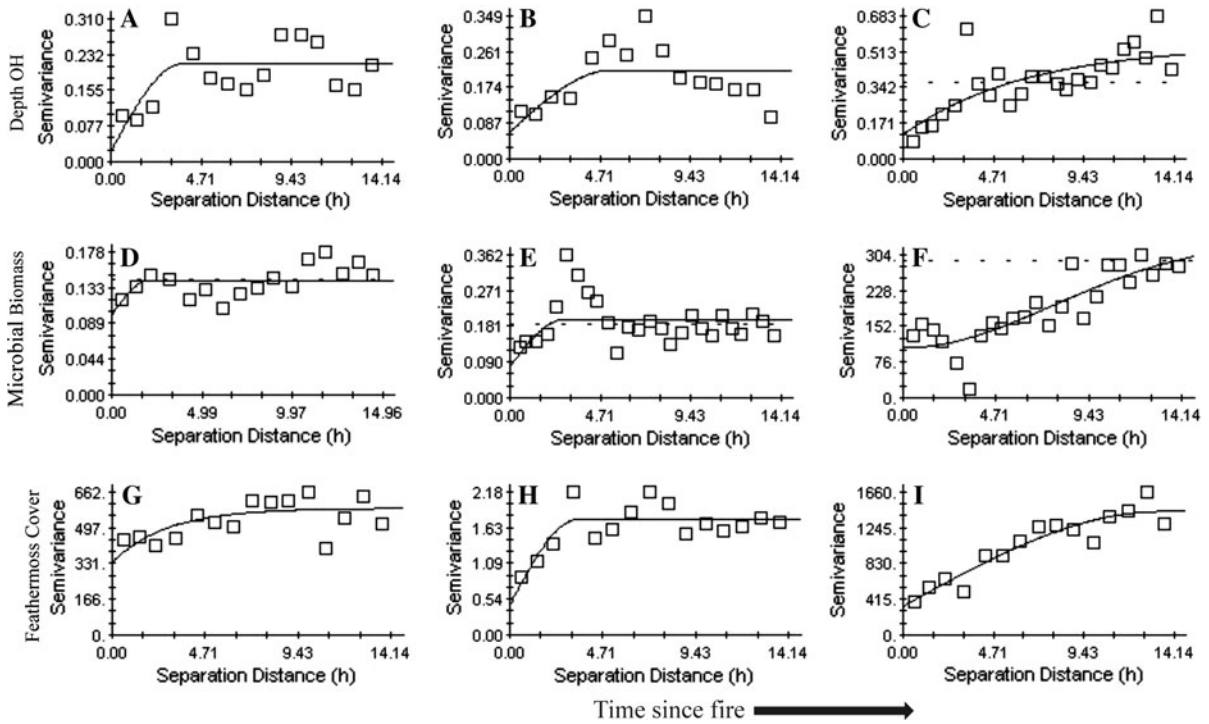

Fig. 2 Semivariograms for the depth of organic horizon (**a**–**c**), microbial biomass (**d**–**f**) and feathermoss cover (**g**–**i**) in a boreal fire chronosequence. Soils were collected from a 1999 (**a**, **d**, **g**), 1987 (**b**, **e**, **h**) and 1920 (**c**, **f**, **i**) wildfire in interior Alaska, USA

Table 6 Pearson correlations between C and N mineralization and gravimetric soil moisture, depth of the organic horizon (OH), total N and C and soil pH

	Soil moisture	Depth of OH	Total N	Total C	pH
1920 Wildfire					
Extractable N ($NO_3^- + NH_4^+$)	**0.33**	**0.24**	**0.60**	**0.63**	−0.02
Lab N mineralization	**0.21**	**0.27**	0.18	0.17	−0.02
Field N mineralization	0.02	−0.06	−0.12	−0.11	0.20
Microbial respiration (initial)	0.02	0.12	**−0.22**	**−0.23**	0.04
Microbial biomass (initial)	**0.76**	**0.42**	**0.65**	**0.59**	−0.21
1987 Wildfire					
Extractable N ($NO_3^- + NH_4^+$)	−0.1	0.27	**0.29**	**0.29**	0.06
Lab N mineralization	−0.17	−0.01	**0.20**	**0.22**	−0.02
Field N mineralization	−0.07	0.18	−0.03	0.02	0.05
Microbial respiration (initial)	**−0.21**	−0.05	**−0.21**	**−0.23**	−0.02
Microbial biomass (initial)	0.48	0.1	**0.54**	**0.50**	0.24
1999 Wildfire					
Extractable N ($NO_3^- + NH_4^+$)	0.04	0.23	**0.24**	**0.23**	−0.07
Lab N mineralization	0.09	−0.05	**0.33**	**0.32**	−0.14
Field N mineralization	−0.03	−0.17	−0.01	0.00	−0.05
Microbial respiration (initial)	−0.16	−0.09	−0.11	−0.14	−0.02
Microbial biomass (initial)	**0.36**	**0.36**	**0.66**	**0.66**	**−0.41**

Bold indicates significance ($p < 0.05$)

Table 7 Parameter estimates and regression coefficients for the generalized least square models between nitrogen (extractable inorganic nitrogen, laboratory and field mineralization rates) and carbon mineralization (microbial respiration and microbial biomass) rates as the dependent variables and gravimetric soil moisture (MC), depth of the organic horizon (Depth), total nitrogen (N), and total carbon (C) as independent variables in a boreal forest chronosequence of interior Alaska

1920 Wildfire	R^2	1987 Wildfire	R^2	1999 Wildfire	R^2
Nitrogen mineralization					
Extractable N = −1.04 + 0.64 MC	0.18	Extractable N = 2.69 − 0.11 MC	0.01	Extractable N = 0.40 + 0.35 MC	**0.12**
Extractable N = 0.92 + 0.35 Depth	0.08	Extractable N = 1.31 + 0.44 Depth	0.07	Extractable N = 1.60 + 0.23 Depth	**0.13**
Extractable N = 0.63 + 3.15 N	0.36	Extractable N = 1.45 + 2.20 N	0.15	Extractable N = 1.40 + 1.61 N	**0.20**
Extractable N = −0.40 + 0.81 C	0.32	Extractable N = 0.77 + 0.60 C	0.13	Extractable N = 1.01 + 0.39 C	**0.21**
Lab N min = −1.69 + 0.78 MC	0.13	Lab N min = 5.13 − 0.42 MC	0.02	Lab N min = 1.19 + 0.01 MC	0.03
Lab N min = 0.47 + 0.46 Depth	0.07	Lab N min = 2.80 + 0.32 Depth	0.01	Lab N min = 0.93 + 0.30 Depth	0.00
Lab N min = 0.73 + 2.37 N	0.10	Lab N min = 2.68 + 2.32 N	0.05	Lab N min = 0.18 + 3.84 N	**0.13**
Lab N min = 0.28 + 0.47 C	0.06	Lab N min = 1.88 + 0.69 C	0.05	Lab N min = −0.16 + 0.71 C	**0.13**
In situ N min = −0.01 + 0.10 MC	0.08	In situ N min = 0.78 − 0.06 MC	0.01	In situ N min = 0.77 − 0.06 MC	0.00
In situ N min = 0.41 − 0.01 Depth	0.00	In situ N min = 0.34 + 0.11 Depth	0.03	In situ N min = 0.65 − 0.15 Depth	0.05
In situ N min = 0.45 − 0.15 N	0.00	In situ N min = 0.57 − 0.07 N	0.00	In situ N min = 0.53 − 0.02 N	0.00
In situ N min = 0.44 − 0.02 C	0.00	In situ N min = 0.50 + 0.02 C	0.00	In situ N min = 0.54 − 0.01 C	0.00
Carbon mineralization					
Mic Respiration = 3.15 + 0.01 MC	0.00	Mic Respiration = 4.01 − 0.26 MC	0.09	Mic Respiration = 3.96 − 0.31 MC	0.04
Mic Respiration = 3.00 + 0.09 Depth	0.02	Mic Respiration = 3.04 − 0.06 Depth	0.00	Mic Respiration = 2.76 − 0.04 Depth	0.01
Mic Respiration = 3.46 − 0.98 N	0.08	Mic Respiration = 3.19 − 0.86 N	0.07	Mic Respiration = 2.82 – 0.38 N	0.01
Mic Respiration = 3.87 − 0.28 C	0.09	Mic Respiration = 3.66 − 0.32 C	0.12	Mic Respiration = 3.05 − 0.16 C	0.07
Mic Biomass = 3.37 + 1.00 MC	**0.69**	Mic Biomass = 5.96 + 0.34 MC	0.10	Mic Biomass = 4.05 + 0.73 MC	**0.25**
Mic Biomass = 7.10 + 0.21 Depth	**0.39**	Mic Biomass = 7.28 + 0.07 Depth	0.00	Mic Biomass = 6.73 + 0.32 Depth	**0.18**
Mic Biomass = 7.00 + 1.80 N	**0.52**	Mic Biomass = 6.77 + 2.10 N	0.26	Mic Biomass = 6.21 + 3.03 N	**0.46**
Mic Biomass = 6.50 + 0.44 C	**0.49**	Mic Biomass = 6.22 + 0.52 C	0.21	Mic Biomass = 5.46 + 0.76 C	**0.50**

Bold R^2 coefficients indicate presence of significant autocorrelation. Otherwise, only the non-spatial component of the model is shown

and likely other aspects of forest succession appeared to homogenize the spatial structure of soil and forest floor characteristics. Or in other words, fire initially creates a patchy mosaic of forest floor cover, from fire hot spots, where high intensity burning exposes mineral soil, to virtually unburned areas with intact mosses and lichens. As time since fire elapses, forest floor cover tends to become more uniform as understory species fill in severely burned areas. This result is consistent with Rodriguez et al. (2009a, b) for a pine forest and Blair (2005) for a wet tropical forest but in contrast to Hirobe et al. (2003) for a dry tropical forest. In the latter, Hirobe et al. (2003) suggested that the decrease in spatial autocorrelation with time after fire was probably due to a stronger influence of the understory plants on soil nutrients in recent burns, while in older stands, the overstory trees had the strongest influence on soil nutrients.

In boreal forests, fire creates patches of burned and unburned materials resulting in multiple small patches of mineral soil and organic matter (litter, feathermosses, or lichen). But as time elapsed after fire, the organic horizon deepened and the feathermoss cover increased, as the former and latter both showed decrease in spatial heterogeneity over time. In our study, the increase in the depth of the organic horizon we measured over time after fire was likely due to the accumulation of litter (e.g., from the F99 to F87 site). Furthermore, this pattern also likely explained the decrease in spatial heterogeneity for microbial biomass (2–10.7 m spatial range) and N mineralization rates (i.e., spatial range <0.5 m to a range of 3.3 m). These results diverge from Smithwick et al. (2005), where they showed ranges of autocorrelation from 5 to 9 m for ammonification, nitrification and mineralization rates, and up to 15 m for total C, soil moisture and dead moss. However, their study was in 1-year old burn and located in a boreal forest site with a deeper residual soil organic horizon (i.e., average of 12 cm but with a range of 3–30 cm). Additionally, higher total C (25 vs. ~12% in this study) and total N (0.8 vs. ~0.4% in this study) and lower understory vegetation cover (~10 vs. ~25% in this study) could also explain the differences between the two studies.

We were not able to detect the effects of wildfire on the spatial distribution of the understory vegetation or forest floor cover, with the exception of feathermosses, because very few species were abundant at any site. However, the effect of fire on the relationship between soil and vegetation abundance appeared to change over time after fire. The number of significant correlations between soil variables and understory abundance decreased as forest succession progressed. For example, we measured stronger correlations between the understory vegetation and N mineralization rates in the young and mid-successional sites than the old site. This lack of correlation in the old site was probably related to the fact that the understory vegetation cover was mainly composed of only two species (~40%). Alternatively, it could also suggest that early in succession higher diversity of understory vegetation had more influence on soil nutrients and that later in succession the organic horizon influence was more important.

The relationship between forest floor cover and soil dynamics also appeared to develop over time after fire. Although absent from the younger sites, negative and positive relationships between feathermosses, lichens, and soil variables existed in the oldest site. Organic horizon thickness, extractable inorganic N, and N mineralization rates were positively correlated with feathermoss abundance but negatively correlated with lichen abundance.

The high numbers of linear and nugget models in this study suggest that the spatial structure for some of the variables we measured extended beyond the scale sampled, while for others the sample grid was simply too coarse to capture the spatial structure. Alternatively, the lack of spatial structure could also be explained by temporal dynamics, in the case of labile variables, such as ammonium or nitrate pools. The spatial structure of one soil variable can change within a year or within a growing season (Ryel et al. 1996; Ehrenfeld et al. 1997; Cain et al. 1999; Guo et al. 2002; Stenger et al. 2002). For example, Ryel et al. (1996) found significant patch structure for two of the three measurements of soil ammonium concentrations. It is not clear, however, whether more integrative variables, such as soil C:N ratio or microbial biomass, would vary as rapidly.

Finally, this study also showed a substantial numbers of non-significant correlations between soil nutrients and vegetation distribution. In contrast to our study and also for a boreal site, Smithwick et al. (2005) found strong correlations between C and N mineralization rates (in situ and lab), and *Ceratodon purpureus*, and forbs species as well. Even though the percentage of mosses (including litter) (73 vs. ~85%

in this study (F99 site)) was relatively similar for both studies, our young site was mostly severely burned. In contrast, in their study *Ceratodon purpureus* was mostly associated with severely burned microsites. This could explain the lack of correlation between C and N mineralization rates, and *C. purpureus* in our study.

Acknowledgements The authors are grateful to Jordan Mayor, Julia Reiskind, Emily Tissier, Oona Takano and Charmaine Wasykowski for field and laboratory assistances. We are also thankful to Ricardo Holdo for statistical assistance. Martin Lavoie received a postdoctoral scholarship from the Fonds québécois de la recherche sur la nature et les technologies (FQRNT). Support was also provided by NSF DEB 0445458 to MCM.

References

Anderson JP, Domsch KH (1978) A physiological method for the quantitative measurement of microbial biomass in soils. Soil Biol Biochem 10:215–221

Beale CM, Lennon JJ, Yearsley JM, Brewer MJ, Elston DA (2010) Regression analysis of spatial data. Ecol Lett 13:246–264

Blair BC (2005) Fire effects on the spatial patterns of soil resources in a Nicaraguan wet tropical forest. J Trop Ecol 21:435–444

Boby LA, Schuur EAG, Mack MC, Verbyla D, Johnstone JF (2010) Quantifying fire severity, carbon and nitrogen emissions in Alaska's boreal forest. Ecol Appl 20: 1633–1647. doi:10.1890/08-2295.1

Bond-Lamberty B, Brown KM, Goranson C, Gower ST (2006) Spatial dynamic of soil moisture and temperature in a black spruce boreal chronosequence. Can J For Res 36:2794–2802

Bugueria S, Pueyo Y (2009) A comparison of simultaneous autoregressive and generalized least squares models for dealing with spatial autocorrelation. Glob Ecol Biogeogr 18:273–279

Cain ML, Subler S, Evans JP, Fortin MJ (1999) Sampling spatial and temporal variation in soil nitrogen availability. Oecologia 118:397–404

Chapin FS III, Viereck LA, Adams P, Van Cleve K, Fastie CL, Ott RA, Mann D, Johnstone JF (2006) Successional processes in the Alaskan boreal forest. In: Chapin FS III, Oswood M, Van Cleve K, Viereck L, Verbyla D (eds) Alaska's changing boreal forest. Oxford University Press, Oxford

Degrandpre L, Gagnon D, Bergeron Y (1993) Changes in the understory of Canadian southern boreal forest after fire. J Veg Sci 4:803–810

Dormann CF, McPherson JM, Araujo MB et al (2007) Methods to account for spatial autocorrelation in the analysis of species distributional data: a review. Ecography 30:609–628

Dyrness CT, Van Cleve K, Levison JD (1989) The effect of wildfire on soil chemistry in four types in interior Alaska. Can J For Res 19:1389–1396

Ellner SP (2001) R version 1.1.1. Bull Ecol Soc Am 82:127–128

Ehrenfeld JG, Han X, Parson WFJ, Zhu W (1997) On the nature of environmental gradients: temporal and spatial variability of soils and vegetation in the New Jersey pinelands. J Ecol 85:785–798

Ettema CH, Wardle DA (2002) Spatial soil ecology. Trends Ecol Evol 17:177–183

Flanagan PW, Van Cleve K (1983) Nutrient cycling in relation to decomposition and organic-matter in taiga ecosystems. Can J For Res 13:795–817

Fortin MJ, Payette S, Marineau K (1999) Spatial vegetation diversity index along a postfire successional gradient in the northern boreal forest. Ecoscience 6:213–214

Gallardo A, Parama R, Covelo F (2005) Soil ammonium vs. nitrate spatial pattern in six plant communities: simulated effect on plant populations. Plant Soil 277:207–219

Gross KL, Pregitzer KS, Burton AJ (1995) Spatial variation in nitrogen availability in three successional plant communities. J Ecol 83:357–367

Gundale MJ, Metlen KL, Fiedler CE, DeLuca TH (2006) Nitrogen spatial heterogeneity influences diversity following restoration in a ponderosa pine forest, Montana. Ecol Appl 16:479–489

Guo D, Mou R, Jones RH, Mitchell RJ (2002) Temporal changes in spatial patters of soil moisture following disturbance: an experiment approach. J Ecol 90:338–347

Guo D, Mou P, Jones RH, Mitchell RJ (2004) Spatial-temporal of soil variable nutrients following experimental disturbance in a pine forest. Oecologia 138:613–621

Havorton JJ, Smith JL, Bolton H Jr, Rossi RE (1995) Evaluating shrub-associated spatial patterns of soil properties in a shrub-steppe ecosystem using multiple-variable geostatistics. Soil Sci Soc Am J 59:1476–1487

Hirobe H, Nobuhito O, Nanae K, Guo-sheng Z, Lin-he W, Ken Y (2001) Plant species effect on the spatial patterns of soil properties in the Mu-us desert ecosystem, Inner Mongolia, China. Plant Soil 234:195–205

Hirobe M, Tokuchi N, Wachrinrat C, Takeda H (2003) Fire history influences on the spatial heterogeneity of soil nitrogen transformations in three adjacent stands in a dry tropical forest in Thailand. Plant Soil 249:309–318

Ives AR, Zhu J (2006) Statistics for correlated data: phylogenies, space, and time. Ecol Appl 16:20–32

Kasischke ES (2000) Effects of climate change and fire on carbon storage in North American boreal forests. In: Kasischke ES, Stocks BJ (eds) Fire, climate change and carbon cycling in the boreal forest. Springer-Verlag, New York, pp 440–452

Kielland K, Olson K, Ruess RW, Boone RD (2006) Contribution of winter processes to soil nitrogen flux in taiga forest ecosystems. Biogeochemistry 81:349–360

Légaré S, Bergeron Y, Paré D (2005) Effect of aspen (*Populus tremuloides*) as a companion species on the growth of black spruce (*Picea mariana*) in the southwestern boreal forest of Quebec. For Ecol Manag 208:211–222

Legendre P, Fortin M-J (1989) Spatial pattern and ecological analysis. Vegetatio 80:107–138

Legendre P, Legendre L (1998) Numerical ecology. 2nd English edition. Elsevier Science BV, Amsterdam

Liu H, Randerson JT, Lidfors J, Chapin III FS (2005) Changes in the surface energy budget after fire in boreal ecosystems of interior Alaska: an annual perspective. J Geophys Res. doi:10.1029/2004JD005158

Mack MC, Treseder KK, Manies KL, Harden JW, Schuur EAG, Vogel JG, Randerson JT, Chapin FS III (2008) Recovery of aboveground plant biomass and productivity after fire in Mesic and dry balck spruce forests of Interior Alaska. Ecosystem 11:209–225

Outeiro L, Aspero F, Ubeda X (2008) Geostatistical methods to study spatial variability of soil cations after a prescribed fire and rainfall. Catena 74:310–320

Richter DD, O'Neill KP, Kasischke ES (2000) Postfire stimulation of microbial decomposition in black spruce (*Picea mariana* L.) forest soils: a hypothesis. In: Kasischke ES, Stocks BJ (eds) Fire climate change and carbon cycling in the boreal forest. Springer-Verlag, New York, pp 197–213

Robertson GP, Crum JR, Ellis BG (1993) The spatial variability of soil resources following long-term disturbances. Oecologia 96:451–456

Robertson GP, Wedin D, Groffman PM, Balir JM, Holland EA, Nadelhoffer KJ, Harris D (1999) Soil carbon and nitrogen availability nitrogen mineralization, nitrification, and soil respiration potentials. In: Robertson GP, Coleman DC, Bledsoe CS, Sollins P (eds) Standard soil methods for long-term ecological research. Oxford University Press, New York, pp 115–142

Rodriguez A, Duran J, Fernandez-Palacios JM, Gallardo A (2009a) Wildfire changes the spatial pattern of soil nutrient availability in *Pinus canariensis* forests. Ann For Sci 66. doi:10.1051/forest/200892

Rodriguez A, Duran J, Fernandez-Palacios JM, Gallardo A (2009b) Short-term wildfire effects on the spatial pattern and scale of labile organic-N and inorganic-N and P pools. For Ecol Manag 257:739–746

Rossi RE, Mulla DJ, Journel AG, Franz EH (1992) Geostatistical tools for modelling and interpreting ecological spatial dependence. Ecol Monogr 62:277–314

Ryel RJ, Caldwell MM, Manwaring JH (1996) Temporal dynamics of soil spatial heterogeneity in sagebrush-wheatgrass steppe during a growing season. Plant Soil 184:299–309

SAS Institute Inc (2003) The SAS system for Windows Version 9.1.2. SAS institute Inc., Cary

Schlesinger WH, Raikes JA, Hartley AE, Cross AF (1996) On the spatial pattern of soil nutrients in desert ecosystems. Ecology 77:364–374

Smith DW (1970) Concentrations of soil nutrients before and after fire. Can J Soil Sci 50:17–29

Smithwick EAH, Mack MC, Turner MG, Chapin FS III, Zhu J, Balser TC (2005) Spatial heterogeneity and soil nitrogen dynamics in a burned black spruce forest stand: distinct controls at different scales. Biogeochemistry 76:517–537

Stenger R, Priesack E, Beese F (2002) Spatial variation of nitrate-N and related soil properties at the plot-scale. Geoderma 105:259–275

Stoyan H, De-Polli H, Bohm S, Robertson GP, Paul EA (2000) Spatial heterogeneity of soil respiration and related properties at the plant scale. Plant Soil 222:203–214

Treseder KK, Mack MC, Cross A (2004) Relationships among fires, fungi, and soil dynamics in Alaskan boreal forests. Ecol Appl 14:1826–1838

Treseder KK, Turner KM, Mack MC (2007) Mycorrhizal responses to nitrogen fertilization in boreal ecosystems: potential consequences for soil carbon storage. Glob Chang Biol 13:78–88

Van Cleve K, Dyrness CT, Viereck LA, Fox JF, Chapin FS III, Oechel W (1983) Taiga ecosystems in interior Alaska. Bioscience 33:39–44

Viereck LA, Dyrness CT, Van Cleve K, Foote MJ (1983) Vegetation, soils, and forest productivity in selected forest types in Interior Alaska. Can J For Res 13:703–720

Vinton MA, Burke IC (1995) Interactions between individual plant species and soil nutrient status in shortgrass steppe. Ecology 76:1116–1133